Physical and Mechanical Properties of Geopolymers with the Addition of NaOH modified Bemban Fiber (Donax Canniformis)

Ninis Hadi Haryanti
Department of Physics, Faculty of Mathematics and Natural Science, Lambung Mangkurat University, South Kalimantan, Indonesia
ninishadiharyanti@ulm.ac.id

Nursiah Chairunnisa
Department of Civil Engineering, Faculty of Engineering, Lambung Mangkurat University, South Kalimantan, Indonesia
nursiah.chairunnisa@ulm.ac.id (corresponding author)

Ade Yuniati Pratiwi
Department of Civil Engineering, Faculty of Engineering, Lambung Mangkurat University, South Kalimantan, Indonesia
ade.pratiwi@ulm.ac.id

Ratni Nurwidayati
Department of Civil Engineering, Faculty of Engineering, Lambung Mangkurat University, South Kalimantan, Indonesia
ratninurwidayat@ulm.ac.id

Wiku Adhiwicaksana Krasna
Department of Civil Engineering, Faculty of Engineering, Lambung Mangkurat University, South Kalimantan, Indonesia
wakrasna@ulm.ac.id

Received: 16 December 2024 | Revised: 23 January 2025 | Accepted: 29 January 2025

 DOI: https://doi.org/10.48084/etasr.9953

ABSTRACT

The increasing demand for sustainable and eco-friendly materials has driven research into natural resource utilization. This study explores the development of geopolymer mortar incorporating fly ash, bemban fiber, and natural kaolin minerals. Due to its hydrophilic nature, bemban fiber requires alkalization treatment to enhance bonding strength within the geopolymer matrix. This research investigates the effect of 3% NaOH alkalization for 2 hours on the fiber's properties. The results indicate that alkalization significantly enhances the physical and mechanical performance of bemban fiber. The optimal composition of 1.5% bemban fiber with a 70:30 metakaolin-to-fly ash ratio improves key properties, including water absorption (2.75%), porosity (5.80%), compressive strength (32.58 MPa), and splitting tensile strength (10.78 MPa). These findings are supported by Fourier Transform Infrared Spectroscopy (FTIR), which confirms geopolymerization through Si-O-Si asymmetric stretching vibrations at 974 cm^{-1}. Additionally, X-Ray Diffraction (XRD) analysis identifies a dominant quartz phase, while Scanning Electron Microscopy (SEM) reveals strong fiber-matrix bonding. This study highlights the potential of bemban fiber-reinforced geopolymers as a sustainable alternative for cement-based materials, promoting green construction practices.

Keywords-geopolymer; bemban fiber; hydrophilic; metakaolin; fly ash

I. INTRODUCTION

The growing demand for environmentally friendly construction materials has led to the development of concrete and geopolymers reinforced with both synthetic and natural fibers [1-6]. Natural fibers offer several advantages, including biodegradability, renewability, relatively high specific strength properties, low cost, and abundance in nature [1]. Geopolymers, in particular, are gaining attention as sustainable materials alternatives to traditional cement-based materials. They can be synthesized from aluminosilicate-rich materials such as metakaolin or industrial by-products like fly ash, combined with alkali activators and water [2]. However, one of the main challenges of incorporating natural fibers into geopolymers is their high lignin and hemicellulose content, which results in poor water resistance and weak adhesion within the matrix [7]. To address this, researchers have explored surface modification techniques, particularly alkalization, to enhance fiber performance. Studies have shown that alkalized natural fibers, such as cotton, sisal, and coconut fibers, improve the compressive strength of fly ash-based geopolymers [8]. Additionally, authors in [9] observed increased tensile strength in metakaolin-based geopolymers reinforced with alkalized bamboo fibers, attributing the improvement to enhanced interfacial bonding within the matrix. Among the various natural fibers, bemban fiber shows significant potential. Bemban (*Donax canniformis*), a member of the Marantaceae family, is also known by its synonyms *Thalia canniformis* and *Donax arundastrum*. It is a green, soft-stemmed plant that grows between 1.5 m and 5 m in height, with segmented stems measuring 1 m to 2.5 m. Bemban is commonly found along riverbanks, in bamboo forests, and in humid regions, where it forms small clusters. Traditionally, bemban fibers have been used for weaving due to their similarity to rattan [10, 11]. In South Kalimantan, Indonesia, bemban is a valuable natural resource, with previous studies exploring its application as a composite reinforcement [12] and as an additive in porous asphalt [13].

Utilizing bemban fiber as an additive in geopolymer mortar is a novel approach. Its beneficial properties, including resistance to extreme temperatures, durability, and rot resistance, make it a promising material for geopolymer applications, particularly in pavement construction [10]. This study investigates the effects of 3% NaOH alkalization treatment on bemban fiber and its impact on the properties of geopolymers. The anticipated outcome is that alkalized bemban fiber will enhance geopolymer characteristics, contributing to the development of more sustainable construction materials while identifying new potential reinforcements for concrete applications.

II. MATERIALS AND METHODS

This research was conducted as a laboratory-based investigation. The primary materials utilized in the geopolymer mortar included bemban fiber, metakaolin, fly ash, silica sand, and alkaline activators.

Metakaolin and bemban fiber, characterized by a porosity of 31.14%, contained 59.30%, SiO_2 and 34.30% Al_2O_3. Fly ash has a higher porosity of 44.06% and contained 31.90% SiO_2 and 6.30% Al_2O_3. Silica sand, used as fine aggregate, had a 5% mud content, an organic content with color rating of 3, and was classified within Zone 4 based on sieve analysis. The alkaline activators consisted of 8 M NaOH and Na_2SiO_3, mixed in a ration of 2.5:1. The mortar composition was a set at a ratio of 65:35, while the paste ratio was 60:40. Geopolymer formulations were prepared using different metakaolin-to-fly ash ratios: 70:30 (G-A), 50:50 (G-B), and 30:70 (G-C). Bemban fiber was incorporated at varying percentages of 0%, 0.5%, 1%, 1.5%, and 2% relative to the total raw material weight. Cylindrical test specimens with diameters of 3.8 cm and 7.6 cm, were prepared and subjected to humid-temperature curing for 28 days. The mix proportions used in the laboratory tests are provided in Table I.

TABLE I. MIX PROPORTION OF SPECIMENS

No	Code of Specimens	Composition (%)		
		Metakaolin	Fly Ash	Bemban Fiber
1	G-A1	70	30	0
2	G-A2	70	30	0.5
3	G-A3	70	30	1.0
4	G-A4	70	30	1.5
5	G-A5	70	30	2.0
6	G-B1	50	50	0
7	G-B2	50	50	0.5
8	G-B3	50	50	1.0
9	G-B4	50	50	1.5
10	G-B5	50	50	2.0
11	G-C1	30	70	0
12	G-C2	30	70	0.5
13	G-C3	30	70	1.0
14	G-C4	30	70	1.5
15	G-C5	30	70	2.0

III. RESULTS AND DISCUSSION

A. Fine Aggregate Inseption

The fine aggregate utilized in this study is silica sand, with test results presented in Table II.

TABLE II. SILICA SAND INSEPTION RESULTS

Type of Testing	Results	Standard Code
Water Content	0.16%	SNI 03-1971-1990
Sludge Content	0.09%	SNI S-04-1989-F
Organic Content	Color 3	SNI 2816-2014
Sieve Analysis	Zone 4	ASTM C136:2012

According to [7], the maximum allowable water content for fine aggregate is 5%, and the tests results confirm that silica sand meets this requirement with a water content of 0.16%. Similarly, the measured mud content (0.09%), is well within the 5% limit specified for fine aggregates. Regarding organic content, color 3 is classified as acceptable for concrete applications, as colors 4-7 are deemed unsuitable [2]. All tests in Table II fulfilled the standard code requirements. According to ASTM C136: 2012, the sieve analysis classifies the silica sand as zone 4, indicating rather fine grains. Additionally, sieve analysis conducted following ASTM C136:2012 indicates that the silica sand falls into Zone 4, meaning it consists of relatively fine grains.

Fine aggregate sand particles pass through sieves with sizes of 4.8 mm (SII.0052:1980), 4.75 mm [8], and 5.0 mm (BS.812:1976) [9], confirming the classification of fine aggregates. For comparison, authors in [10] analyzed silica sand from PT. Sukabumi Silica (Kp. Mekar Alam, Desa Sekarwangi, Cibadak) and reported a water content of 1.15% and mud content of 1.67%. Similarly, [11] studied silica sand from Samarinda, recording a water content of 1.50% and mud content of 3.27%, with an organic content rating of color 3. Further validation of silica sand particle gradation was conducted using SEM (Scanning Electron Microscopy) analysis to assess morphology and particle size distribution, as illustrated in Figures 1 and 2.

B. Silica Sand Morphology

The surface morphology of silica sand, as depicted in Figure 1, reveals a variety of shapes and sizes, making it suitable as a row material for geopolymers.

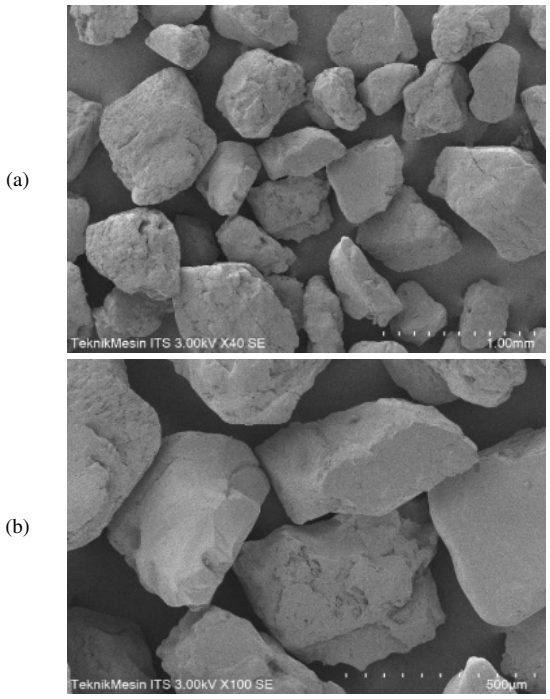

Fig. 1. Surgace mmorphology of silica sand at different magnifications: (a) 40x, (b) 100x.

The SEM images indicate that the silica sand particles exhibit a uniform morphology, with irregular and flat-oval shapes. These observations align with findings from [12], which also reported irregularly shaped silica sand particles. The SEM analysis further provides data on particle size distribution, as illustrated in Figure 2. The average particle diameter of the silica sand is 389.92 µm, which is relatively fine and consistent with the Zone 4 classification from the sieve analysis. This particle size is notably smaller than the 3.267 mm average size reported in [13]. Additionally, the organic components detected in the silica sand, as summarized in Table II, are further confirmed by Energy Dispersive X-ray Spectroscopy (EDX) analysis, with results presented in Figure 3 and Table III.

The EDX analysis confirms that silica sand primarily consists of oxygen (56.63%) and silicon (41.54%) by weight, with smaller proportions of aluminum (Al) and iron (Fe). These results indicate that silica sand is a silicate material with a high silicon dioxide (SiO_2) content. The relatively low iron content suggests that the silica sand sample is highly pure and largely free from contamination by other elements [14]. This purity, combined with its favorable physical properties, makes silica sand well-suited for use as a filler in geopolymer compositions. Additionally, its sufficient silicon and aluminum content ensures effective activation in the geopolymerization process.

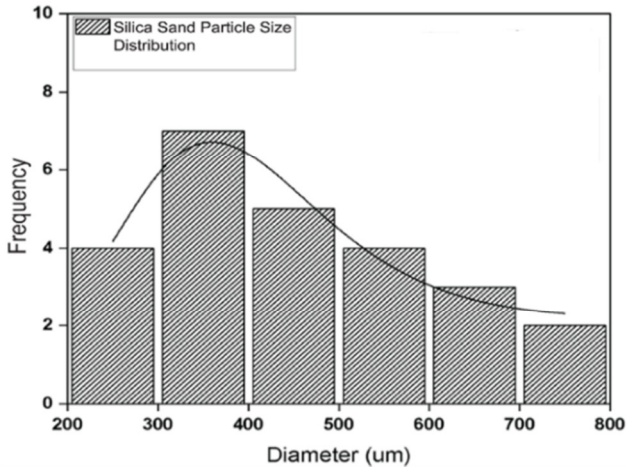

Fig. 2. Silica sand particle size distribution (source: SEM data processing results with ImageJ software).

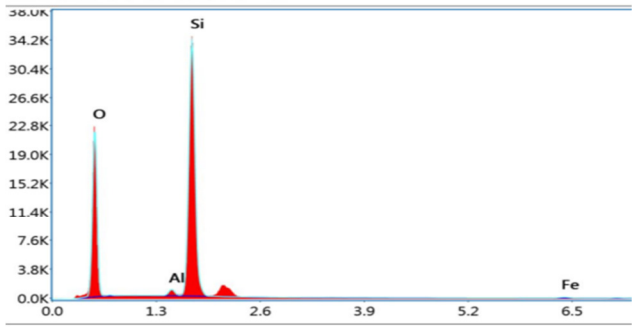

Fig. 3. Silica sand element spectra (source: silica sand EDX test results).

TABLE III. SILICA SAND ELEMENT CONTENT

Element	Weight (%)	Atomic (%)
O	56.63	69.77
Si	41.54	29.15
Al	1.14	0.83
Fe	0.69	0.24

Source: EDX test results of silica sand.

C. Physical Characteristics of Hybrid Geopolymer

Water absorption testing was conducted following the methodology outlined in [15]. This test evaluates the percentage of water absorbed by each specimen. Figure 4 presents the water absorption and porosity values of hybrid geopolymers, ranging from 2.75% to 13.93%.

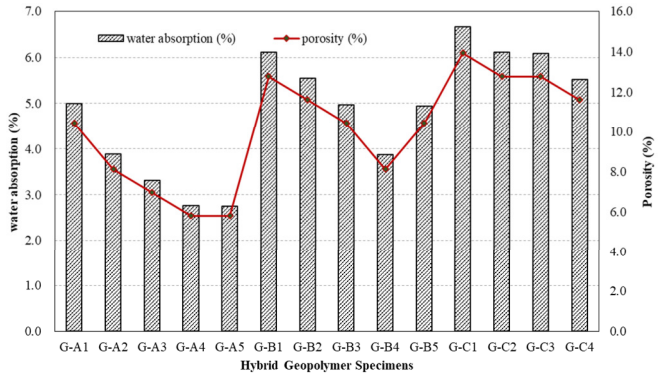

Fig. 4. Water absorption and porosity of all specimens.

Water absorption is directly proportional to the porosity of the geopolymer, meaning that higher water absorption indicates a greater number of pores. As illustrated in Figure 4, some specimens exhibit relatively high-water absorption, particularly those with higher fly ash content. This behavior is attributed to differences in material adhesion, influenced by the physical and chemical properties of the constituent materials. According to [14, the increased water absorption in fly ash-rich specimens is due to the higher porosity of fly ash compared to metakaolin. A similar trend is observed in geopolymer porosity, where metakaolin-dominant mixtures generally have lower porosity than those with higher fly ash composition. The increase porosity in fly ash-based geopolymers is related to its active SiO_2 content [15]. Additionally, SiO_2 plays a crucial role in geopolymer adhesion, and specimens with higher metakaolin content tend to have smaller pores, which is beneficial for geopolymer strength.

The addition of bemban fiber significantly influences water absorption and porosity. As fiber content increases, both water absorption and porosity decrease, reaching an optimal level at 1.5% fiber content. Beyond this threshold, water absorption and porosity increase again, likely due to excessive fiber content creating voids and cavities within the matrix. Bemban fiber contributes to reduced water absorption and porosity because alkalized fibers become more hydrophobic, thereby improving fiber-matrix adhesion. The G-B4 sample demonstrated the most favorable results, with a water absorption capacity of 2.75% and porosity of 5.80%. These values comply with the SNI 03-0691-1996 standard, which sets a maximum allowable water absorption of 10%. Since porosity directly impacts the mechanical properties of geopolymers, where higher porosity leads to lower density and strength, it is crucial to optimize fiber content.

Figure 5 illustrates the compressive strength and splitting tensile strength of hybrid geopolymer specimens. Specimens with higher metakaolin content exhibit greater compressive strength compared to fly ash-based. This is attributed to the higher SiO_2 and Al_2O_3 content in metakaolin. During geopolymerization, the SiO_2 and Al_2O_3 in metakaolin react with the activator solution, forming silicate and aluminosilicate polymer chains that contribute to the material's strength and stiffness. As noted by [16], silicates enhance hardness and strength, while alumina imparts special properties such as refractoriness. Furthermore, the calcination of kaolin transforms it into metakaolin, enhancing its reactivity with NaOH activators and improving geopolymer properties. The incorporation of 0.5% to 2% bemban fiber further increases the compressive strength of the geopolymer.

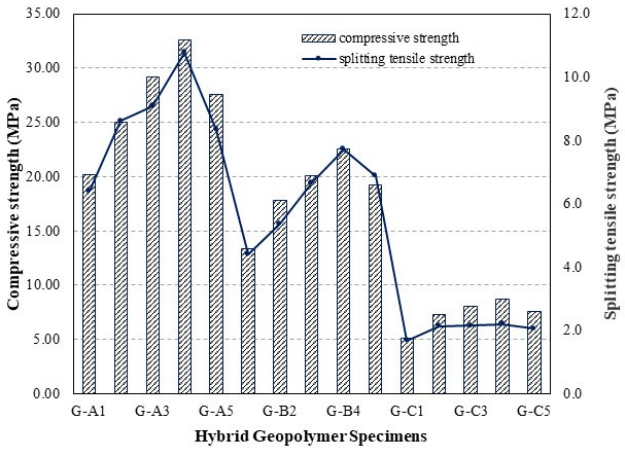

Fig. 5. Splitting and compressive strength of hybrid geopolymer specimens.

Increasing bemban fiber content enhances compressive strength, with the optimum strength observed at 1.5% fiber across all compositions. This aligns with findings from authors in [17], who reported that fiber addition can increase mechanical strength by 30–70%. However, exceeding the optimal fiber limit leads to a decline in strength, as excessive fiber content creates voids within the geopolymer matrix, increasing porosity and reducing overall material integrity. The alkalization treatment of bemban fibers enhances their bonding with the matrix, improving adhesive properties [18]. This is further validated by SEM analysis, which confirms better fiber-matrix interaction. Additionally, splitting tensile strength follows a similar trend, increasing alongside compressive strength, as illustrated in Figure 6.

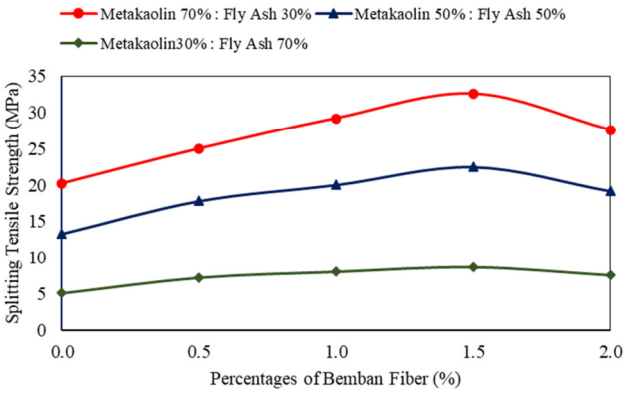

Fig. 6. Splitting tesndile strength test of hybrid geopolymer specimen.

Splitting tensile strength is directly proportional to compressive strength; as compressive strength increases, splitting tensile strength also improves. Typically, the splitting tensile strength of geopolymers ranges between 9% and 15% of

their compressive strength. The incorporation of bemban fiber enhances splitting tensile strength, as the high tensile strength of alkalized fibers allows stress transfer from the geopolymer matrix to the fibers through an improved fiber-matrix interface [19]. Test results indicate that geopolymer mortar with increasing fiber content exhibits improved tensile strength, reaching an optimal fiber content of 1.5%. Beyond this limit, workability decreases, negatively impacting mechanical properties. Furthermore, fiber-reinforced geopolymer specimens demonstrate superior load-bearing capacity compared to specimens without fiber reinforcement. The observed increase in both compressive and tensile strength results from matrix-fiber interactions, specifically involving the Si-O-Si-O-Al-O polymer chains, which chemically react with hydroxyl (OH) groups in cellulose to form hydrogen bonds [20]. This conclusion is further supported by FTIR microstructural analysis, as illustrated in Figure 7.

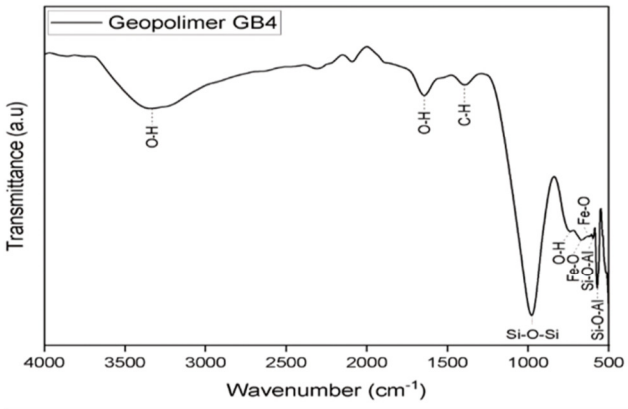

Fig. 7. Spectra IR geopolymer G-B4.

The absorption band at 3430 cm^{-1} corresponds to O-H stretching vibrations produced by water molecules during 28-day moist curing. The 1646 cm^{-1} band indicates geopolymer hydration [21]. The 1397 cm^{-1} absorption is attributed to C-H stretching vibrations, confirming the presence of cellulose from bemban fibers within the geopolymer matrix. The 738 cm^{-1} band corresponds to O-H bending vibrations, indicative of kaolinite, where Al (III) occupies octahedral positions, forming Al-OH derived from metakaolin [22]. The 688 cm^{-1} and 621 cm^{-1} bands correspond to Fe-O stretching vibrations, confirming the presence of iron (Fe) from fly ash. Additionally, most octahedral sites in metakaolin are occupied by Mg (II) or Fe (II) [23]. The 598 cm^{-1} and 570 cm^{-1} absorption bands are associated with Si-O-Al bending vibrations, formed during the geopolymerization process [24]. Geopolymer formation is characterized by the presence of an absorption band between 1200-950 cm^{-1}, which corresponds to the asymmetric stretching vibrations of Si-O-Si and Si-O-Al bonds [17]. A strong and sharp absorption peak at 974 cm^{-1} confirms the geopolymerization process. This observation aligns with previous studies [16, 20], which reported that geopolymers consistently form within this absorption region. The 974 cm^{-1} peak specifically results from the reaction between bemban fiber, metakaolin, and fly ash, with shifts in the wave number indicating ongoing geopolymerization reactions. The geopolymerization process is further confirmed by X-ray diffraction (XRD) data, as illustrated in Figure 8.

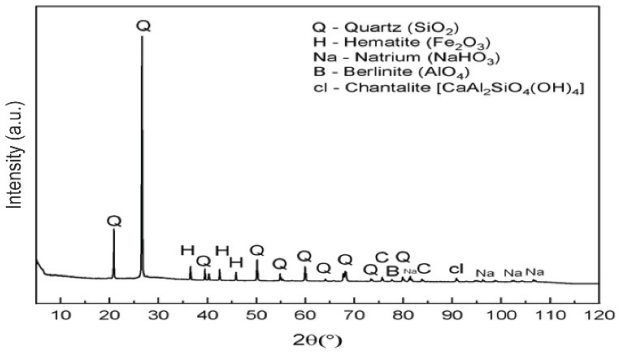

Fig. 8. XRD doffractogram of geopolymer G-B4.

The XRD diffractogram confirms that the geopolymer exhibits a crystalline structure, with distinct peaks at 2θ = 20.84°, 26.60°, 36.53°, 39.44°, 40.27°, 42.40°, 45.77°, 50.13°, 54.85°, 64.00°, 67.71°, 73.43°, 75.62°, 77.86°, 80.08°, 81.14°, 81.71°, 91.09°, 96.20°, 102.55°, and 106.59°. According to authors in [24], peaks within the 20°–33° 2θ range are characteristic of geopolymer materials, confirming the successful formation of a geopolymer phase. The geopolymer is primarily composed of quartz, with hematite derived from Fe, sodium from the activator, berlinite from metakaolin, and chantalite, a combination of alumina-silica-calcium. This XRD analysis is consistent with FTIR results (Figure 7), which show strong Si-O-Si bond absorption, further verifying the successful polymerization of silica and alumina. Additionally, the high silicon (Si) and oxygen (O) content aligns with EDX elemental analysis results (Table IV), confirming the silicate-based composition of the geopolymer. Finally, the role of bemban fiber in geopolymer microstructure is further examined through Scanning Electron Microscopy (SEM) analysis.

SEM testing was conducted on specimens that underwent compressive strength testing to observe the internal morphology of the geopolymer cracks. The presence of bemban fibers in the geopolymer, presented in Figure 9(a), indicates that even after compressive strength testing, the bemban fibers remain intact. This suggests a strong bond between the fibers and the geopolymer matrix. This is attributed to the adhesive properties resulting from the NaOH alkalization treatment, which removes ineffective components, as evidenced by the FTIR test results of the bemban fibers. Additionally, the homogeneity of the matrix, illustrated in Figure 9(b), demonstrates that metakaolin, fly ash, and silica sand can bond effectively and fill each other. The geopolymer matrix results from the reaction of silica and alumina monomers that form polymers. Geopolymers consist of raw materials comprising silica and alumina, as shown in Table IV.

The EDX analysis confirms that the hybrid geopolymer primarily consists of oxygen (O), silicon (Si), and sodium (Na). The high O and Si content originates from the bemban fiber, metakaolin, and fly ash which serve as the geopolymer's base materials. The presence of Na confirms the use of NaOH as an activator, consistent with findings in [17]. Other elemental

components identified in the geopolymer include aluminum (Al) content of 9.12% which is derived from metakaolin and fly ash, iron (Fe) content of 2.20% which is present due to the constituents, calcium (Ca) which indicates a minor presence of fly ash in the sample, potassium (K) and magnesium (Mg) which naturally occurring from the geopolymer's raw materials.

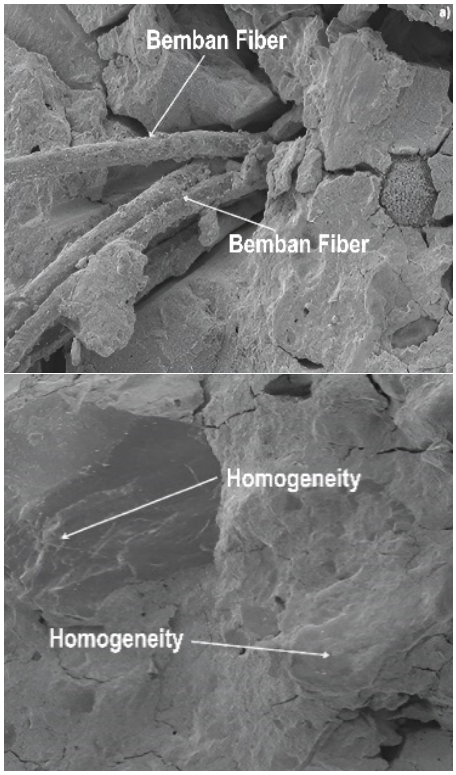

Fig. 9. SEM morphology of geopolymer G-B4: (a) presence of berban fiber, (b) the homogeneity.

TABLE IV. ELEMENT CONTENT OF HYBRID GEOPOLYMER G-B4

Element	Weight (%)	Atomic (%)
O	44.27	57.13
Si	25.75	18.93
Na	16.79	15.08
Al	9.12	6.98
Fe	2.20	0.81
Ca	1.21	0.62
K	0.33	0.18
Mg	0.32	0.27

Given its potential application in pavement structures, the thermal stability of the hybrid geopolymer is analyzed using the DTG-DSC (Differential Thermal and Thermogravimetric) test, as illustrated in Figure 10. The thermal events occurring during the heating process at temperatures ranging from 30°C to 550°C, at a heating rate of 10°C/min. Key thermal events observed during the analysis include an endothermic process at temperatures between 59°C and 133°C, with a power of 21.3 mW·s/mg, indicating the rate of energy change relative to mass, followed by a mass reduction of 2.40% on the TG curve, which is attributed to the evaporation of water. This process requires heat energy to overcome the attractive forces between water molecules and convert them into vapor [26]. Subsequently, at the peak temperature of 280°C, an exothermic process occurs, releasing heat during the formation of the geopolymer matrix, accompanied by a mass loss of 2.81% on the TG curve. This process is influenced by various factors, including alkali concentration, material ratio, and reaction conditions [20], and is associated with phase transitions in mineral composition [16].

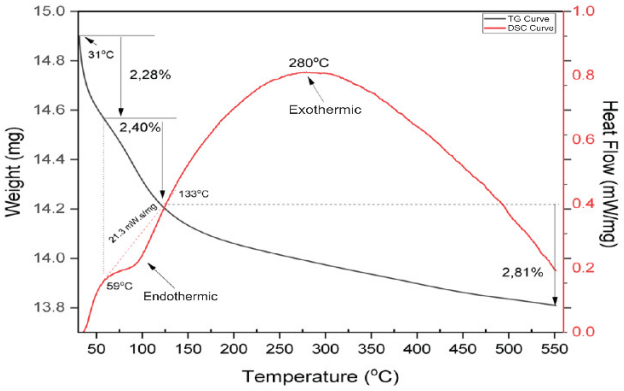

Fig. 10. Thermal curve of hybrid gepolymer G-B4.

According to [27], metakaolin-based geopolymers exhibit high thermal stability, typically losing 13% of their mass at 550°C. However, in this study, the mass loss is significantly lower at 7.49%, suggesting enhanced thermal resistance. Geopolymers derived from fly ash lost 19.8% of their mass when heated to 550°C [27]. This indicates that geopolymers possess better stability than cement mortar, which can lose over 25% of its mass at 550°C [28]. Furthermore, the inclusion of natural fibers contributes to the thermal properties of geopolymers, with reports indicating that the mass loss of fly ash geopolymers with added cotton fibers above 300°C is due to the dihydroxylation of chemically bound water and the decomposition of cotton fiber [29]. The geopolymers in this study demonstrate considerable resistance to temperature changes, indicating their potential application as rigid pavements due to their interaction with solar heat. This can be confirmed by other previous research which conclude that mortar geopolymer using natural and synthetic fiber can develop strength of geopolymer [30].

IV. CONCLUSION

This study investigated the development of geopolymer mortar incorporating bemban fiber, fly ash, and metakaolin as an eco-friendly alternative to conventional cement-based materials. The results demonstrate that alkalization treatment (3% NaOH for 2 hours) significantly enhances the physical and mechanical properties of bemban fiber, improving its bonding strength within the geopolymer matrix.

The optimal composition was identified as 1.5% bemban fiber with a 70:30 metakaolin-to-fly ash ratio, yielding low water absorption (2.75%) and porosity (5.80%), improving material durability, while enhanced mechanical performance, with compressive strength of 32.58 MPa and splitting tensile

strength of 10.78 MPa. These improvements are confirmed by FTIR analysis, which identifies geopolymerization through Si–O–Si asymmetric stretching vibrations at 974 cm^{-1}, and XRD analysis, which reveals a dominant quartz phase. SEM imaging further verifies the strong interfacial bonding between bemban fibers and the geopolymer matrix. Additionally, thermal analysis (TG-DSC) demonstrates the geopolymer's high thermal stability, with lower mass loss (7.49%) at 550°C compared to conventional cement mortars. This indicates the material's potential for high-temperature applications, such as pavement construction.

This research highlights the potential of utilizing locally available materials-such as bemban fiber, fly ash, and metakaolin-to develop sustainable, cement-free geopolymer mortar. By eliminating cement, this approach contributes to carbon footprint reduction, aligning with the principles of sustainable infrastructure development. To further assess the viability of bemban fiber-reinforced geopolymers, long-term performance tests will be conducted to evaluate durability and environmental resistance under real-world exposure conditions.

V. FUTURE WORK

The findings highlight the sustainability benefits of replacing cement with locally available materials, reducing carbon emissions and promoting green construction practices. Future research should focus on:

- Long-term durability assessments under environmental exposure.
- Further optimization of fiber content for maximum performance.
- Expanded applications in infrastructure projects, including pavement and structural elements.

By integrating natural fibers and industrial byproducts, this study contributes to sustainable infrastructure development, providing a viable alternative to traditional construction materials.

ACKNOWLEDGEMENT

The authors would like to thank Lambung Mangkurat University for its support through the DRTPM Grant Program by LPPM ULM under contract number 1043/UN8.2/PG/2024.

REFERENCES

[1] Y. C. Choi, "Hydration and internal curing properties of plant-based natural fiber-reinforced cement composites," *Case Studies in Construction Materials*, vol. 17, Dec. 2022, Art. no. e01690, https://doi.org/10.1016/j.cscm.2022.e01690.

[2] M. M. Camargo, E. Adefrs Taye, J. A. Roether, D. Tilahun Redda, and A. R. Boccaccini, "A Review on Natural Fiber-Reinforced Geopolymer and Cement-Based Composites," *Materials*, vol. 13, no. 20, Jan. 2020, Art. no. 4603, https://doi.org/10.3390/ma13204603.

[3] S. Farhan Mushtaq *et al.*, "Effect of Bentonite as Partial Replacement of Cement on Residual Properties of Concrete Exposed to Elevated Temperatures," *Sustainability*, vol. 14, no. 18, Jan. 2022, Art. no. 11580, https://doi.org/10.3390/su141811580.

[4] S. Ahmad, A. Shah, A. Nawaz, and K. Salimullah, "Shear Strengthening of Corbels with Carbon Fibre Reinforced Polymers (CFRP)," *Materiales de Construcción*, vol. 60, no. 299, pp. 79–97, Sep. 2010, https://doi.org/10.3989/mc.2010.50009.

[5] K. Rodsin *et al.*, "Behavior of steel clamp confined brick aggregate concrete circular columns subjected to axial compression," *Case Studies in Construction Materials*, vol. 16, Jun. 2022, Art. no. e00815, https://doi.org/10.1016/j.cscm.2021.e00815.

[6] P. Joyklad, A. Nawaz, and Q. Hussain, "Effect of Fired Clay Brick Aggregates on Mechancal Properties of Concrete," *Suranaree Journal of Science & Technology*, vol. 25, no. 4, 2018, Art. no. 349.

[7] G. Silva, S. Kim, R. Aguilar, and J. Nakamatsu, "Natural fibers as reinforcement additives for geopolymers – A review of potential eco-friendly applications to the construction industry," *Sustainable Materials and Technologies*, vol. 23, Apr. 2020, Art. no. e00132, https://doi.org/10.1016/j.susmat.2019.e00132.

[8] K. Korniejenko, E. Frączek, E. Pytlak, and M. Adamski, "Mechanical Properties of Geopolymer Composites Reinforced with Natural Fibers," *Procedia Engineering*, vol. 151, pp. 388–393, Jan. 2016, https://doi.org/10.1016/j.proeng.2016.07.395.

[9] R. A. Sá Ribeiro, M. G. Sá Ribeiro, K. Sankar, and W. M. Kriven, "Geopolymer-bamboo composite – A novel sustainable construction material," *Construction and Building Materials*, vol. 123, pp. 501–507, Oct. 2016, https://doi.org/10.1016/j.conbuildmat.2016.07.037.

[10] A. Syarief, A. A. Basyir, and A. Nugraha, "Pengaruh Orientasi Serat Dan Waktu Alkalisasi Pada Laminates Composite Polyester-Serat Bemban (Donax Canniformis) Terhadap Kekuatan Bending, Impact Dan Bentuk Patahan," *Info-Teknik*, vol. 22, no. 2, pp. 209–226, Dec. 2021, https://doi.org/10.20527/infotek.v22i2.12387.

[11] D. Harsono, "Sifat Fisis dan Mekanis ANyaman Bamban (Donax canniformis) dengan Bahan Stabilisator Peg 1000 dan Tanin Kulit Akasia," *Jurnal Riset Industri Hasil Hutan*, vol. 7, no. 2, pp. 23–30, 2014.

[12] S. M. F. Al-Idrus, "Perbandingal Komposit Polyester Sebat Bemban (Donax Canniformis), Timbaran, Dan Bilaran Terhadar Kekuatan Impak dan Bending," M.S. Thesis, Universitas Islam Kalimantan MAB, Kalimantan, Indonesia, 2020.

[13] A. Alviyanda and C. S. Sipayung, "Studi Batuan Asal (Provenance) Batupasir Formasi Simpangaur Daerah Way Krui, Lampung," *Journal of Science and Applicative Technology*, vol. 7, no. 1, pp. 26–34, May 2023, https://doi.org/10.35472/jsat.v7i1.1086.

[14] E. Hariska, K. Kasman, and S. Ulum, "Analisis Sifat Fisik dan Mekanik Beton Geopolymer Dengan Pengikat Berbahan Dasar Fly Ash PLTU Mpanau," *Gravitasi*, vol. 18, no. 1, pp. 24–35, Jul. 2019, https://doi.org/10.22487/gravitasi.v18i1.13307.

[15] K. V. Setiani, "Karakterisasi Material Refraktori dengan Bahan Dasar Fly Ash dan Metakaolin," 2021.

[16] R. F. Giese, "Kaolin Minerals: Structures and Stabilities," in *Hydrous Phyllosilicates (exclusive of micas)*, 2nd ed., vol. 19, Chelsea, MI, USA: BookCrafters, Inc., 1991, pp. 29–66.

[17] S. Anwar and E. Kusumastuti, " Pemanfaatan Serat Pohon Pisang Dalam Sintesis Geopolimer Abu Layang Batubara," *Indonesian Journal of Chemical Science*, vol. 5, no. 1, May 2016, https://doi.org/10.15294/ijcs.v5i1.9170.

[18] N. A. Latip, A. H. Sofian, M. F. Ali, S. N. Ismail, and D. M. N. D. Idris, "Structural and morphological studies on alkaline pre-treatment of oil palm empty fruit bunch (OPEFB) fiber for composite production," *Materials Today: Proceedings*, vol. 17, pp. 1105–1111, Jan. 2019, https://doi.org/10.1016/j.matpr.2019.06.529.

[19] Y.-C. Ding, Y.-S. Fang, and T.-W. Cheng, "Preparation and characterization of vitrified slag/geopolymers for construction and fire-resistance applications," *Materials and Structures*, vol. 49, no. 5, pp. 1883–1891, May 2016, https://doi.org/10.1617/s11527-015-0620-8.

[20] X. Liu *et al.*, "Thermal stability and microstructure of metakaolin-based geopolymer blended with rice husk ash," *Applied Clay Science*, vol. 196, Oct. 2020, Art. no. 105769, https://doi.org/10.1016/j.clay.2020.105769.

[21] N. Toniolo *et al.*, "Fly-ash-based geopolymers: How the addition of recycled glass or red mud waste influences the structural and mechanical properties," *Journal of Ceramic Science and Technology*, vol. 8, no. 3, pp. 411–420, 2017.

[22] B. B. Kenne Diffo, A. Elimbi, M. Cyr, J. Dika Manga, and H. Tchakoute Kouamo, "Effect of the rate of calcination of kaolin on the properties of

metakaolin-based geopolymers," *Journal of Asian Ceramic Societies*, vol. 3, no. 1, pp. 130–138, Mar. 2015, https://doi.org/10.1016/j.jascer.2014.12.003.

[23] Y.-S. Li, J. S. Church, and A. L. Woodhead, "Infrared and Raman spectroscopic studies on iron oxide magnetic nano-particles and their surface modifications," *Journal of Magnetism and Magnetic Materials*, vol. 324, no. 8, pp. 1543–1550, Apr. 2012, https://doi.org/10.1016/j.jmmm.2011.11.065.

[24] O. Ayeni, A. P. Onwualu, and E. Boakye, "Characterization and mechanical performance of metakaolin-based geopolymer for sustainable building applications," *Construction and Building Materials*, vol. 272, Feb. 2021, Art. no. 121938, https://doi.org/10.1016/j.conbuildmat.2020.121938.

[25] U. Rattanasak, K. Pankhet, and P. Chindaprasirt, "Effect of chemical admixtures on properties of high-calcium fly ash geopolymer," *International Journal of Minerals, Metallurgy, and Materials*, vol. 18, no. 3, pp. 364–369, Jun. 2011, https://doi.org/10.1007/s12613-011-0448-3.

[26] A. Nikolov, "Characterization of Geopolymer Based on Fayalite Waste and Metakaolin with Standard Consistence," *Comptes rendus de l'Académie bulgare des Sciences*, vol. 74, no. 10, pp. 1461–1498, 2021, https://doi.org/10.7546/CRABS.2021.10.05.

[27] M. A. Villaquirán-Caicedo, R. M. de Gutiérrez, S. Sulekar, C. Davis, and J. C. Nino, "Thermal properties of novel binary geopolymers based on metakaolin and alternative silica sources," *Applied Clay Science*, vol. 118, pp. 276–282, Dec. 2015, https://doi.org/10.1016/j.clay.2015.10.005.

[28] L. Alarcon-Ruiz, G. Platret, E. Massieu, and A. Ehrlacher, "The use of thermal analysis in assessing the effect of temperature on a cement paste," *Cement and Concrete Research*, vol. 35, no. 3, pp. 609–613, Mar. 2005, https://doi.org/10.1016/j.cemconres.2004.06.015.

[29] T. S. Alomayri, "Development and characterization of cotton and cotton fabric reinforced geopolymer composites," PhD dissertation, Imaging and Applied Physics, Curtin University, Feb. 2015.

[30] A. A. Amiruddin, M. Tumpu, P. R. Rangan, R. Irmawaty, B. Bakri, and Mansyur, "A Potential Pozzolanic Material consisting of Rice Straw Ash and Fly Ash for Geopolymer Mortar Production-based Cementitious System," *Engineering, Technology & Applied Science Research*, vol. 14, no. 6, pp. 18189–18198, Dec. 2024, https://doi.org/10.48084/etasr.8703.